

# Adaptive Barrier Coverage Using Software Defined Sensor Networks

Linghe Kong, Siyu Lin, Weiliang Xie, Xiaoyu Qiao, Xi Jin, Peng Zeng, Wanli Ren, and Xiao-Yang Liu

**Abstract**—This paper investigates the adaptive barrier coverage system in wireless sensor networks, where multiple mobile sensor nodes collaboratively move based on cloud computing. This system aims to adaptively maintain a barrier coverage surrounding a dynamic zone, such as nuclear leakage area and toxic gas area. Since such a zone is usually dangerous and invisible, it is necessary to monitor and track its boundary for detecting unwanted people nearby and warning them. Existing studies on mobile barrier coverage mainly focus on static zones, which cannot directly apply into dynamic zones because their movement strategies are not flexible with dynamics. To address such a problem, we propose a novel adaptive barrier coverage system. The challenge is to effectively maintain the barrier when the change of dynamic zone is unpredictable. The proposed system leverages the software defined concept, in which the mobile sensor nodes execute the local sensing tasks and the cloud computes the real-time optimal strategy to control the movements of nodes. Extensive simulations based on large-scale real trace demonstrate the efficiency and the efficacy of the proposed system.

**Index Terms**—Wireless sensor networks, mobile computing, barrier coverage.

## I. INTRODUCTION

WITH the dramatic growth in industrial development, the natural environment is easily destroyed by pollution, such as inappropriate deposition of industrial waste, sewage, toxic gas emission, chemical spills and *etc.* [25]. Thus, the monitoring of such pollutants is imperative to prevent environmental and people disasters. To avoid irrelevant people penetrating the dangerous zone, deploying mobile

Manuscript received April 2, 2016; revised April 30, 2016; accepted May 7, 2016. Date of publication May 11, 2016; date of current version September 16, 2016. This work was supported in part by the China Post-Doctoral Science Foundation under Grant 2014M560334 and Grant 2015T80433, in part by the National Natural Science Foundation of China under Grant U1534201, Grant 61501023, Grant 61303202, and Grant U1334202, in part by the Fundamental Research Funds for the Central Universities under Grant 2015RC032, and in part by the State Key Laboratory of Rail Traffic Control and Safety under Grant RCS2015K011. The associate editor coordinating the review of this paper and approving it for publication was Dr. Yin Zhang. (*Corresponding author:* Siyu Lin.)

L. Kong and X.-Y. Liu are with the Department of Computer Science and Engineering, Shanghai Jiao Tong University, Shanghai 200240, China (e-mail: linghe.kong@sjtu.edu.cn; yanglet@sjtu.edu.cn).

S. Lin and W. Ren are with the School of Electronic and Information Engineering, Beijing Jiaotong University, Beijing 100044, China (e-mail: sylin@bjtu.edu.cn; wanli\_ren@126.com).

W. Xie and X. Qiao are with the Technology Innovation Center, China Telecom Corporation Ltd., Beijing 102209, China (e-mail: xiewl@ctbri.com.cn; qiaox@ctbri.com.cn).

X. Jin and P. Zeng are with the Shenyang Institute of Automation, Chinese Academy of Sciences, Shenyang 110016, China (e-mail: jinxj@sia.cn; zp@sia.cn).

Digital Object Identifier 10.1109/JSEN.2016.2566808

sensors at the boundary of the zone to detect and warn them, commonly known as barrier coverage, becomes critical.

The barrier coverage topic has attracted extensive concerns in the research community of wireless sensor networks (WSNs) [19]. Many valuable efforts have been made for barrier coverage [2], [14] in the literature. Existing works, no matter the sensor nodes are mobile [1], [3], [16] or not [13], [21], [26], mainly focus on static zones, *e.g.*, the border line. Nevertheless, the pollution, such as oil spills, is usually dynamic, whose shape and position are time-varying. When the zone begins to move, the state-of-the-art solutions fail to maintain a barrier coverage. This is our motivation to study the *adaptive barrier coverage* (ABC) for dynamic zone.

Compared with the conventional barrier coverage, ABC not only inherits all properties such as intrusion detection, but also has a new feature that ABC can transform itself according to the change of dynamic zone. For supporting this new feature, the mobile sensor nodes should have the ability of sensing both the outside intruders and the boundary of the zone.

There are three major challenges in maintaining barrier coverage for dynamic zone. First, the pollution zone is dynamic and its change is unpredictable. Second, with the limited number of mobile sensor nodes, the monitoring quality of ABC should be maximized in the dynamic case. This quality is commonly characterized by the number of barriers  $K$  [14]. Third, since the batteries of a mobile sensor nodes are always constrained, the travel distance of nodes should be minimized for energy saving. Briefly, the adaptive barrier coverage problem aims to maintain a dynamic barrier while maximizing its monitoring performance and minimizing the energy consumption.

To tackle these challenges, we leverage the software defined concept [11], where a cloud-based architecture [4], [28], [29] is used to control the mobility of sensor nodes. The software defined sensor networks can resort to not only the local sensing knowledge but also the cloud-based intelligence to adjust the movement strategy, so that the barrier coverage service can be enhanced in complex environments.

In this paper, we study the adaptive barrier coverage for dynamic zone as follows:

First, we formulate the  $K$ - $D$  ABC problem to maximize the number of barriers  $K$  and to minimize the total travel distance  $D$  of sensor nodes. We derive the theoretical maximum  $K$  when the number of sensor nodes  $n$  is given. After that, we discuss the optimal movement pattern of sensor nodes to maintain the maximum  $K$  while achieving the minimum  $D$ .

Second, the theoretical optimum cannot be achieved in practice because of two reasons. (i) The change of the pollution zone is unpredictable, and (ii) every sensor node senses only partial information of the boundary. To approach the optima, mobile sensor nodes report their positions and sensing information to the cloud via LTE/5G communication system [5], and the cloud computes the collaborative movement strategy to control all nodes. The core concept is to form sensor nodes as an elastic barrier wrapping the dynamic zone, which is inspired by an elastic band wrapping around an object.

Finally, we conduct extensive simulations based on real trace collected from toxic red tide populations in the Western Gulf of Maine. Performance results show that the proposed system closely approaches the optimum  $K$ - $D$  barrier coverage.

The contributions of this paper are as follows.

- We study the practical problem on adaptive barrier coverage to monitor the dynamic zone such as industrial pollution.
- We derive the theoretical optimal  $K$ - $D$  adaptive barrier coverage for both high monitoring quality and low energy consumption.
- We develop a software defined sensor system that the cloud controls the sensor nodes to retain  $K$ - $D$  adaptive barrier coverage corresponding to the dynamic zone. The proposed solution is demonstrated to perform well in a realistic setting through trace driven simulations.

## II. RELATED WORK

Barrier coverage facilitates the applications of intrusion detection and border surveillance in real world. We classify the existing barrier coverage works into three categories.

### A. Stationary Nodes for Static Zones

Most existing works fall in this category, in which the barrier coverage is formed by stationary nodes in order to protect static zones or objects. The research of barrier coverage is firstly introduced in [14]. Then, a distributed algorithm is proposed to locally determine the formation of barrier coverage [2]. Recently, a bulk of works design the barrier coverage in different directions such as line-based barrier in [21], curve-based barrier in [10], belt-based barrier in [23], directional camera based barrier in [27], and probabilistic barrier coverage in [3].

### B. Mobile Nodes for Static Zones

With the development of robotic techniques [8], mobile sensor nodes start to be utilized in real applications [6]. Several innovative works fall in this category, in which mobile sensor nodes form the barrier surrounding static zones. For example, the automatic barrier formation mechanism is designed in [12] with omni-directional sensors. Nevertheless, only a few sensors have omni-directional sensing ability. Consequently, Wang et al propose an optimal solution for sectorial sensing area [24], such as cameras, to achieve  $K$ -barrier coverage. Furthermore, to guarantee the monitoring quality even the number of sensor nodes is inadequate, a periodic scheduling is investigated to control the movement [9].

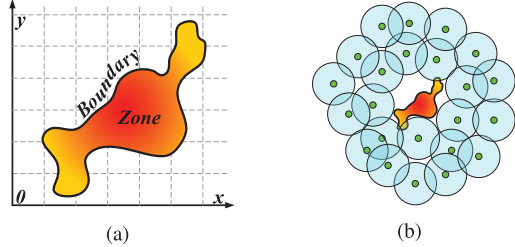


Fig. 1. (a) The model of dynamic zone is an area with a closed boundary on a 2D plane. (b) Mobile sensor nodes form a barrier coverage wrapping the dynamic zone.

Specially, for energy saving, lots of solutions are proposed to trade off the monitoring quality and the lifetime of the barrier coverage [7], [17].

### C. Mobile Nodes for Dynamic Zones

In this category, the zones begin to move. Thus, mobile sensor nodes have to be adopted in order to keep wrapping the dynamic zones. Conventional methods for static zones cannot maintain the barrier coverage for such dynamic zones. Research in this category is little. For example, in [15], mobile full coverage is investigated to detect the intruder in dynamic zones. However, full coverage costs more sensor nodes than barrier coverage. Hence, this paper pay attention to the problem of adaptive barrier coverage for dynamic zones.

## III. PROBLEM STATEMENT

In this section, we present the models, the metrics, and the formulation of the adaptive barrier coverage (ABC) problem.

### A. Models

The ABC problem considers the dynamic zone (*e.g.*, oil spill areas), intruders and sensor nodes moving on a two-dimensional plane during the given time period  $T$ . We divide  $T$  into discrete time slots and denote the beginning of  $T$  as  $t = 0$ . The distance between two points  $a_1$  and  $a_2$  is denoted by  $d(a_1, a_2)$ . If  $A_1$  and  $A_2$  are two areas in the plane,  $d(A_1, A_2) = \min\{d(a_i, a_j) | \forall a_i \in A_1, \forall a_j \in A_2\}$ .

1) *Dynamic Zone Z*: A dynamic zone is an area enclosed by a closed boundary as shown in Fig. 1, which moves and deforms on the 2D plane. We are interested in the time-varying boundary of  $Z$ , denoted by  $\beta(t)$ , and do not care about its internal change. The change of  $\beta(t)$  is unknown during  $T$ .

2) *Intruder I*: An intruder (intruder) is a person or an animal that is desired to be detected when it moves towards the dynamic zone  $Z$ . The intruder could be a point, a changeable area or several separate areas on the 2D plane. The appearance of intruders is unknown in advance.

3) *Safety Distance  $\epsilon$* : It is the shortest allowed distance between an intruder and the dynamic zone. An intruder is required to be detected at least one sensor node when  $d(Z, I) \leq \epsilon$ . The value of  $\epsilon$  is set according to the requirement of diverse applications.

4) *Mobile Sensor Nodes  $s_i$ :* In order to detect all intruders, a complete barrier coverage wrapping the dynamic zone is necessary. So that any intruder could be immediately detected when it goes across the barrier region. The mobile sensor nodes are promising candidates to collaboratively build such a barrier. We assume that there are totally  $n$  sensor nodes, denoted by  $s_i, i = 1, \dots, n$ . The maximum velocity of these sensor nodes is  $v_s$ . Every node can obtain its position by GPS devices. A node can sense both the boundary of  $Z$  and the intruder  $I$  within its sensing range. We adopt the widely used disk model [2], [6] to describe the coverage area, where every sensor node  $s_i$  has an equal sensing range  $r_s$ .

5) *Barrier Coverage:* A barrier coverage is defined as a virtual closed belt region surrounding the dynamic zone  $Z$ , which is built by the sensing coverage of all sensor nodes. An example of the barrier coverage is shown in Fig. 1. An intruder cannot reach  $Z$  without crossing this barrier.

### B. Metrics

The goal of the mobile sensor nodes is to maintain an adaptive barrier coverage with the change of the dynamic zone. Two major metrics need to be considered in our design.

1) *Number of Barriers  $K$ :* An ABC has  $K$  barriers if and only if an intruder is detected by at least  $K$  nodes when it crosses the belt region to  $Z$ . An ABC with  $K$  barriers is referred to  $K$ -ABC. Increasing  $K$  can produce a higher monitoring quality for intruder detection.

2) *Total Travel Distance  $D$ :* In a given period, the sum of travel distances of all nodes is denoted by the total travel distance  $D$ . Let  $\mu_i(t_1, t_2)$  denote the distance travelled by the sensor node  $s_i$  from  $t_1$  to  $t_2$ . The total travel distance is given by

$$D(0, T) = \sum_{i=1}^n \mu_i(0, T). \quad (1)$$

It is critical to reduce the total travel distance of mobile sensor nodes because the mobile nodes have only limited battery.

### C. Problem Formulation

1) *The  $K$ -D Adaptive Barrier Coverage Problem:* Given  $n$  mobile sensor nodes, this problem studies how to collaboratively move these nodes with the objective to minimize the total travel distance under the constraint of maximize the number of barriers at any time. Mathematically, the  $K$ -D ABC problem is formulated by

$$\begin{cases} \text{Objective: } \min D(0, T), \\ \text{Subject to: } \max(K). \end{cases} \quad (2)$$

## IV. THEORETICAL ANALYSIS

In this section, we derive the theoretical maximum  $K$  when a dynamic zone is given, and then we discuss the optimal movement pattern for the mobile sensor nodes in order to achieve  $\max(K)$  and  $\min(D)$ .

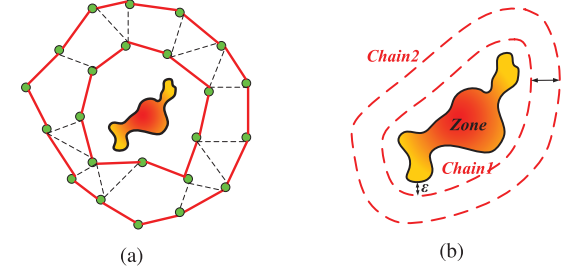


Fig. 2. (a) An example of coverage graph. The sensor nodes form two vertex-disjoint chains. (b) A two-chain barrier wraps a dynamic zone. The minimum distance between Chain1 and the zone is  $\epsilon$ . The distance between two chains is the same everywhere.

### A. Maximum Number of Barriers $K$

Since the dynamic zone is time-varying and the number of sensor nodes is fixed, the maximum number of barriers  $K$  consequentially changes. Intuitively,  $K$  becomes smaller when the size of dynamic zone grows up.

*Theorem 1:* The maximum  $K$  is achieved when all sensor nodes are evenly distributed on the  $\epsilon$ -convex hull of the dynamic zone. The real-time maximum  $K$  is  $\frac{2nr_s}{\phi(\beta(t)) + 2\pi\epsilon}$ , where  $\phi()$  is the operator to obtain the length of convex hull.

*Proof:* We prove Theorem 1 by introducing four lemmas.

*Lemma 1:* Sensor nodes form a  $K$ -ABC if and only if there are  $K$  vertex-disjoint chains in the coverage graph.

The coverage graph  $\mathcal{G} = \langle V, E \rangle$  consists of the vertex set  $V$  and the edge set  $E$ , where  $V$  is the nodes' positions and  $E$  is the connected relationship when the distance between any two sensor nodes is less than  $2r_s$ . An example of  $\mathcal{G}$  is shown in Fig. 2. One barrier is defined as a closed sequence of edges and contains the zone inside. Multiple barriers are separate if they have no shared vertex. Lemma 1 can be directly proved in the same way as [14, Th. 4.2].

Since the number of sensor nodes  $n$  is fixed and any edge between two sensor nodes is no longer than  $2r_s$ , the total length of all barriers is no longer than  $2nr_s$ . Thus, the maximum  $K$  will be achieved when the length of every barrier is minimized.

*Lemma 2:* The shortest barrier is the  $\epsilon$ -convex hull of a dynamic zone.

According to the basic theory in convex analysis [20], in a 2D plane, the smallest polygon  $\Omega$ , which can contain an area  $Z$ , is  $Z$ 's convex hull. This convex hull has not only the smallest area but also the smallest length.

We denote the convex hull of the zone as CH and the  $\epsilon$ -convex hull as  $\epsilon$ -CH. The  $\epsilon$ -convex hull is defined as a closed chain satisfying: (1) The CH is contained inside the  $\epsilon$ -CH; (2) the distance between  $\epsilon$ -CH and CH is  $\epsilon$  everywhere, i.e.,  $d(CH, \epsilon\text{-CH}) = \epsilon$ . From [20], we can have that the length of  $\epsilon$ -convex hull is  $\phi(\beta(t)) + 2\pi\epsilon$  if the length of the convex hull is  $\phi(\beta(t))$ .

At a certain time point, the dynamic zone can be treated as a static area. If we set  $\epsilon = 0$ , the shortest barrier is the convex hull of  $Z$ . If we set  $\epsilon > 0$ , the shortest barrier is the  $\epsilon$ -convex hull of the dynamic zone.

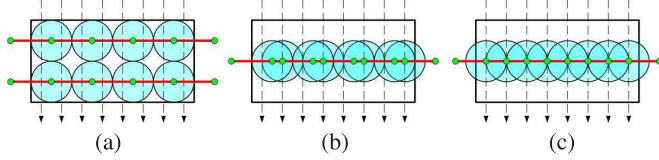


Fig. 3. (a) In a segment of barrier coverage, mobile sensor nodes distribute on two chains, where  $K = 2$ . (b) Mobile sensor nodes distribute on one chain, where  $K = 2$ . (c) Mobile sensor nodes evenly distribute on one chain, where  $K = 2$  as well.

**Lemma 3:** The maximum number of barriers  $K$  is achieved when the dynamic belt is the chain of  $\epsilon$ -convex hull, and the value of maximum  $K$  is  $\lfloor \frac{2nr_s}{\phi(\beta(t))+2\pi\epsilon} \rfloor$ .

Forming sensor nodes into several separated chains is an available solution. As shown in Fig. 2, two convex-hull-like chains are formed by sensor nodes, where the distance between Chain1 and Chain2 is  $m$ . The Chain1 is the  $\epsilon$ -convex hull. And the length of the Chain2 is  $\phi(\beta(t))+2\pi\epsilon+2\pi m$ . If we shrinks the Chain2 to be the same as Chain1, there are still two chains and  $\pi m/r_s$  nodes could be saved for Chain2.

We find that  $K$  is determined by the number of chains, but it is independent to the distribution of chains. As illustrated in Fig. 3(a) and Fig. 3(b), no matter two chains are separated or overlapped, the values of  $K$  remain 2. In both scenarios, any intruder crossing the barriers will be detected at least by two sensor nodes.

When all chains take the shortest length, they are completely overlapped on the  $\epsilon$ -convex hull. The length of adaptive barrier therefore is  $\phi(\beta(t))+2\pi\epsilon$ . In this case, the value of  $K$  is maximized, where  $K = \frac{2nr_s}{\phi(\beta(t))+2\pi\epsilon}$ . Such a dynamic chain could achieve  $K$ -ABC if any point on the chain is covered by at least  $K$  sensor nodes, i.e., there are  $K$  sensor nodes in any segment with length of  $2r_s$  on the  $\epsilon$ -convex hull.

**Lemma 4:** It is a sufficient condition for maximizing the number of barriers  $K$  that the sensor nodes are evenly distributed on the  $\epsilon$ -convex hull of the dynamic zone.

As shown in Fig. 3(c), all sensor nodes are evenly distributed on the  $\epsilon$ -convex hull, which results in the distance between any two closest neighbors as  $\Delta = \frac{\phi(\beta(t))+2\pi\epsilon}{n}$ . Hence, there are  $K = \frac{2r_s}{\Delta} = \frac{2nr_s}{\phi(\beta(t))+2\pi\epsilon}$  nodes in any segment with length of  $2r_s$ , and the maximum  $K$  in Lemma 3 is achieved.

Then, Theorem 1 is proved. ■

According to Theorem 1, towards maintaining the maximum  $K$  in dynamic case, the sensor nodes should change their positions and always evenly distribute on the  $\epsilon$ -convex hull. However, the  $\epsilon$ -convex hull changes when the dynamic zone deforms. Therefore, the sensor nodes should move correspondingly and form the dynamic  $\epsilon$ -convex hull.

#### B. Minimum Total Travel Distance $D$

Besides maximizing the value of  $K$ , we then study how to minimize the total travel distance of mobile sensor nodes. It is challenging to achieve the minimum  $D$ . On one hand, there are countless possible directions and paths to move for every sensor node. On the other hand, all sensor nodes should collaboratively move in order to maintain the maximum  $K$ .

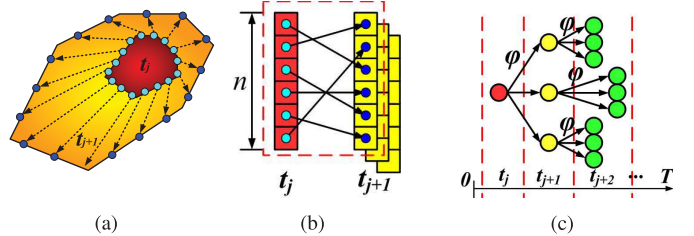


Fig. 4. (a) Sensor nodes move to candidate positions on the  $\epsilon$ -convex hull from  $t_j$  to  $t_{j+1}$ . (b) Finding the movements with minimum  $D$  at two consecutive stages can be converted to a weighted bipartite matching problem. (c) Finding the movements with minimum  $D$  during whole  $T$  can be converted to a multiple-stage weighted bipartite matching problem.

We consider the motion of the dynamic zone as a multi-staged process and divide the time into discrete time slots. Theoretically, we derive the minimum total travel distance when the motion track of the dynamic zone is ideally given.

**Theorem 2:** The  $K$ -D ABC problem can be reduced to a multiple-stage minimum weighted bipartite matching problem.

**Proof:** For analysis, we resort to two consecutive stages  $t_j$  and  $t_{j+1}$ . Fig. 4 shows an example of nodes' movements from the stage  $t_j$  to  $t_{j+1}$ . In order to keep the maximum  $K$ , the sensor nodes should be evenly distributed on the  $\epsilon$ -convex hull at both the stage  $t_j$  and  $t_{j+1}$ . At each stage, there may be  $\varphi$  different combinations of the nodes' positions and all these combinations can achieve the maximum  $K$ . Given a specific positioning of the nodes at stage  $t_{j+1}$ , the movements of sensor nodes are shown in Fig. 4. It is intuitive that each node has to be assigned to one of  $n$  candidate places at stage  $t_{j+1}$ . Such a movement assignment can be essentially considered as a weighted bipartite matching. Each edge is associated with a weight representing the movement distance that a node moves from the position at the stage  $t_j$  to the assigned position at the stage  $t_{j+1}$ .

Then, the movement of the sensor nodes during whole  $T$  can be considered as a multi-staged weighted bipartite matching process. As shown in Fig. 4, each circle represents a specific position assigned to all sensor nodes. Each arrow represents a possible path combination of the nodes from the previous stage to the next stage. From the stage  $t_j$  to  $t_{j+1}$ , since one circle can have  $\varphi$  different path combinations to maintain  $K$ , there are  $\varphi$  different edges. Then Theorem 2 is proved. ■

With Theorem 2, we have a brute force algorithm to compute the minimum total travel distance  $D$  in the  $K$ -D ABC problem. For each edge in Fig. 4, there are  $n!$  possible path combinations. Thus, the total search space is  $O(\varphi^T n^T)$ . The following corollary gives a much faster algorithm to compute the minimum total travel distance.

**Corollary 1:** The minimum total travel distance  $D$  in the  $K$ -D ABC problem can be computed with the complexity of  $O(\varphi^T n^{3T})$ .

**Proof:** From the first stage to the last stage during whole  $T$ , there are in total  $\varphi^T$  combinations of possible path combinations of the sensor nodes. Finding the result of an weighted bipartite matching problem is known as the assignment problem, which could be solved by using a modified shortest path search in the augmenting path algorithm. If the Bellman-Ford algorithm is used, the running time becomes

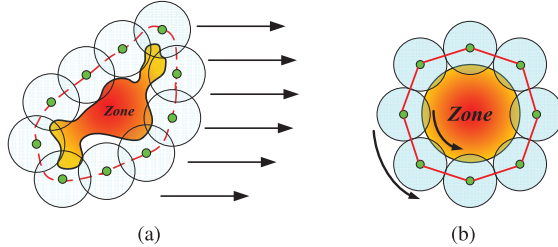


Fig. 5. (a) Translation movement of the dynamic zone. (b) Rotation movement of the dynamic zone.

$O(V^2 E) = O(n^4)$ , or the edge cost can be shifted with a  $O(V^2 \log(V) + VE) = O(n^3)$  running time using the Dijkstra algorithm and Fibonacci heap. Such classical algorithms significantly decrease the computational complexity. Finally, the total complexity is  $O(\varphi^T n^{3T})$ . ■

In order to maintain the convex hull and minimize the total travel distance, we summarize the movement patterns for mobile sensor nodes as:

- When the zone moves as a rigid, the sensor nodes keep the  $\epsilon$ -convex hull shape and move together with this zone.
- When the zone grows or shrinks its size, the sensor nodes scale the  $\epsilon$ -convex hull shape with the zone.
- When the zone rotates, the sensor nodes keep the  $\epsilon$ -convex hull shape but do not rotate with the zone.

The change of the dynamic zone can be considered as the combination of translation, scaling and rotation. For the translation case as shown in Fig. 5, all sensor nodes have to move the same distance as the zone in order to maintain the maximum  $K$ . The same reason applies for the scaling case. Nevertheless, for the rotation case, the sensor nodes are able to decrease the travel distance by forming a chain which does not rotate strictly with the zone. In Fig. 5, we show an ideal example that the zone is round and only rotates counterclockwise. We compare two movement patterns. In the first pattern, all sensor nodes remain stationary, and in the second pattern, all sensor nodes rotate together with the zone. Both patterns achieves the maximum  $K$ , but the first pattern has a zero travel distance. Hence, an energy-efficient movement pattern is to move with as less as barrier's rotation.

## V. ADAPTIVE BARRIER COVERAGE SYSTEM

In the last section, we discuss the theoretical maximum  $K$ -barrier coverage and the minimum  $D$  movement pattern. However, the theoretical analysis cannot be easily achieved in real world because of two reasons. First, the theoretical results are derived when the movement of the dynamic zone is given. In practice, it is impossible to know the future of dynamic zone. Second, every sensor node can know only partial information of the zone. Nevertheless, the optimal movement pattern requires the global information of the zone.

To tackle these two practical issues, we propose a software defined adaptive barrier coverage system, which resorts to the concept of the software defined networking [11]. The movement strategy is not consolidated in the mobile sensor nodes. Instead, a centralized controller is utilized to control the movements of sensor nodes in real-time. If any new

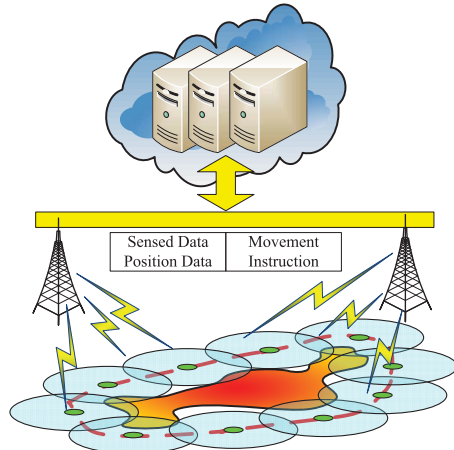


Fig. 6. The cloud-based architecture.

situation is discovered in real world, the movement strategy can be easily adjusted by software method at the controller.

To design such a system, the core components include the cloud-based architecture and the movement strategy controller.

### A. Cloud-Based Architecture

The cloud-based architecture consists of two parts: multiple sensor nodes and a cloud center. These two parts are connected by the LTE/5G communication system as shown in Fig. 6.

**Mobile Sensor Nodes:** The major task for mobile sensor nodes is to sense the change of the dynamic zone and detect the intruders. These nodes report their sensed data and positions to the cloud periodically. In addition, if any intruder is detected, they will report this case to the cloud immediately and warn the intruder not to approach the dangerous zone. The sensor nodes can move on the surface of land and sea. However, their movement is controlled by the cloud.

**Cloud:** The cloud takes in charge of the computing task. Based on the feedback information from the sensor nodes, the cloud runs the basic algorithm to compute the optimal next positions of sensor nodes. Then, it sends the movement instructions to all sensor nodes.

The cloud-based architecture benefits from the following advantages.

- Although every sensor node only senses partial information of the zone, the cloud has a global view because of the information collection from all sensor nodes.
- The cloud has the strong computing capability, which can compute the optimal next positions for all sensor nodes quickly.

The distributed architecture is an option for adaptive barrier coverage system, in which sensor nodes can exchange information via wireless communications (such as WiFi or ZigBee) and determine the movements themselves. Compared with the distributed architecture, the centralized cloud-based architecture may increase the infrastructure cost. However, the cloud-based architecture provides better quality of service including higher  $K$ , lower  $D$  (because of global view), and lower response time (because of strong computing capability).

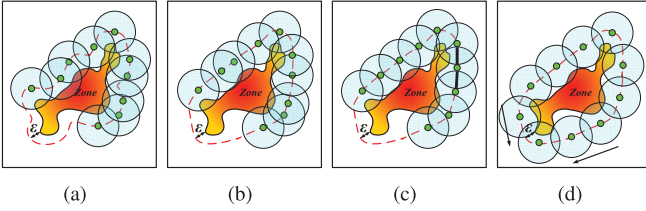


Fig. 7. (a) Sensor nodes distributing on the  $\epsilon$ -boundary extension of the dynamic zone. (b) Sensor nodes move to the positions on the  $\epsilon$ -convex hull. (c) Sensor nodes move to the position of middle of two closest neighbors. (d) Sensor nodes move towards the direction where no neighbor exists.

### B. Movement Strategy Controller

Using the cloud-based architecture, the *movement strategy controller* determines the movement strategy to maintain the barrier coverage for various real environments such as 3D terrain and obstruction. In addition, if meeting new environment, sensors can sense it and report it to the cloud. Then, the controller learns the new environment and generate corresponding new strategy. This design resorts to the similar design in new policy generation in software defined networks (SDN) [18].

Then, we propose a basic movement algorithm for sensor nodes in the usual 2D plane case. All the other movement strategies for complex environments can be plugged into the controller, whose designs are our future work.

The basic movement strategy is named by *barrier maintenance algorithm* (BMA) as shown in Alg. 1, which is operated at the controller by default.

In order to achieve  $K$ - $D$  adaptive barrier coverage, imitating an elastic band wrapping around an object is a potential strategy. First, an elastic band always forms the convex hull of an object. Second, an elastic band can effectively decrease the travel distance by ignoring rotation and concave deformation of the dynamic zone. Leveraging the principles of elastic band, we design the barrier maintenance algorithm.

To collaboratively control the mobile sensor nodes, we introduce the virtual force into BMA. In the community of sensor networks, Zou and Chakrabarty [30] firstly propose the concept of virtual force, which is produced by measuring the distance between nodes. Using virtual force in our BMA can imitate the tension among elastic molecules. Thus, the sensor nodes are desired to adaptively form the  $\epsilon$ -convex hull and evenly distribute on this hull.

Based on the virtual force, we design four steps for movement control.

*Step 1:* The sensor nodes should move close to the boundary of the dynamic zone and stay on the  $\epsilon$ -boundary extension.

By following Step 1, the sensor nodes can be distributed on the  $\epsilon$ -boundary extension as shown in Fig. 7(a).

*Step 2:* A sensor node should maintain the internal angle being no more than  $180^\circ$ . A sensor node with its closest left and right neighbors can form two angles. The internal angle is defined as the angle facing to the boundary.

By following Step 1 and 2, the sensor nodes can be distributed on the  $\epsilon$ -convex hull as shown in Fig. 7(b).

---

**Algorithm 1** Barrier Maintenance Algorithm (BMA Calculates the Next Position of  $s_i$ , Which Is Executed in the Cloud Center.)

---

```

Input: the sensing range  $r_s$ , the warning distance  $\epsilon$ ; the
position of a sensor node  $p_{s_i}$ ; the position of this node's
left neighbor  $p_{s_{i-1}}$  and right neighbor  $p_{s_{i+1}}$ ; the distance
 $d(p_{s_i}, Z)$ 
while True do
     $p \leftarrow p_{s_i}$ ; //  $p$  is the next position that  $s_i$  will move to
    if  $s_i$  has two closest neighbors (left and right)
         $p_1 \leftarrow$  the middle position of two neighbors;
        if  $d(p_{s_i}, Z) < r_s$ 
             $p_2 \leftarrow q: d(Z, q) = \epsilon$  and  $d(p_{s_{i+1}}, q) = d(p_{s_{i-1}}, q)$ ;
             $p \leftarrow d(Z, p_2) > d(Z, p_1)? p_2 : p_1$ ;
        else  $p \leftarrow p_1$ ;
    else if  $s_i$  has only one neighbor
         $p \leftarrow q: d(p_{s_{i\pm 1}}, q) = 2r_s$  and  $d(Z, q) = \epsilon$ ;
        if  $p \neq p_{s_i}$ 
            Move to  $p$ ;
    end while

```

---

*Step 3:* A sensor node should move to the point that has the same distance to its two closest left and right neighbors in order to achieve the even distribution on the  $\epsilon$ -convex hull.

In Fig. 7(c), the result of the previous three steps is shown.

*Step 4:* A sensor node should move towards the direction where there is no neighbor.

This step allows the virtual force to pull the sensor nodes towards the vacant direction along the  $\epsilon$ -convex hull in order to form a complete barrier. Fig. 7(d) illustrates this effect and the resulting chain.

Combining the four steps, the pseudo-code of BMA is given in the algorithm table. When the positions of left and right neighbors are updated or the change of boundary is sensed, a sensor node needs to move to a new position. The next position  $p$  should satisfy  $d(p, Z) = \epsilon$  and  $d(s_i, s_{i-1}) = d(s_i, s_{i+1})$ , which indicates the perpendicular bisector of the left and right neighbors. If this  $p$  constructs an internal angle larger than  $180^\circ$ , i.e., against Step 2, the next point must change to the middle position of two neighbors. If this sensor node has only one neighbor, it moves to the reverse direction of this neighbor.

This algorithm is executed round-by-round. At every round, BMA computes the next position from the 1-st sensor node to the  $n$ -th node while setting the sensor node's left and right neighbors are fixed. The cloud computes several rounds of BMA until all next positions are converged. These next positions are treated as the final movement instructions.

Each sensor node equipped with the LTE/5G transceiver, sending their position and sensed data to the cloud, and receiving the movement instructions. Since the size of reported data and movement instructions are very small, the LTE/5G is adequate to afford these communications in real-time. It is possible that the link quality is not good enough to connect the cloud in certain time slot, which results in some delay.

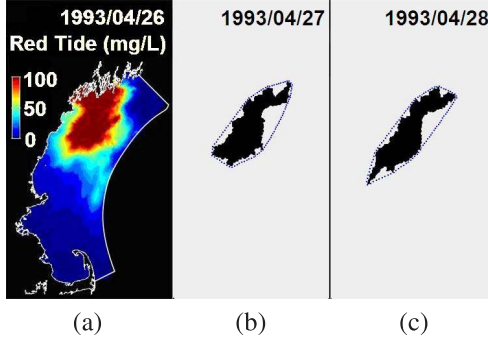


Fig. 8. (a) Red tide data on 1993/04/26. (b) Result of the adaptive barrier coverage wrapping the red tide on 1993/04/27. (c) Result of the adaptive barrier coverage wrapping the red tide on 1993/04/28.

However, once the link is connected again, the cloud can re-organize the sensor node into the barrier in the next time slot.

### C. Discussion

Two practical constraints are needed to be discussed.

When the dynamic zone grows too large, the given  $n$  sensor nodes may not guarantee even  $K = 1$ . It will happen when the length of the  $\epsilon$ -convex hull is larger than  $2nr_s$ . In this case, the cloud needs to decide whether assign more sensor nodes to maintain the barrier.

In the ideal 2D plane scenario, the BMA requires that the velocity of mobile sensor node  $v_s$  should be larger than  $v_z\sqrt{1 + (\frac{2\pi}{n})^2}$ , where  $v_z$  is the maximum velocity of the boundary of the dynamic zone. Consider the worst case when the boundary moves outwards at the velocity  $v_z$ . In this case, a sensor node has to move outward, and meanwhile adjusts its position on the  $\epsilon$ -CH. The length of the convex hull increases by no more than  $2\pi v_z$ . Since  $n$  sensor nodes evenly distribute on the  $\epsilon$ -CH, the average distance for every sensor node is no more than  $2\pi v_z/n$ . By combining the two kinds of distances, the aggregated travel distance of the sensor node is  $\sqrt{v_z^2 + (\frac{2\pi v_z}{n})^2}$ .

## VI. PERFORMANCE EVALUATION

In this section, we conduct trace-driven simulations to evaluate the proposed adaptive barrier coverage system.

### A. Simulation Settings

To evaluate the proposed system under a realistic setting, we utilize the real trace data of toxic red tide populations collected from the Western Gulf of Maine [22]. One example of the trace data is visualized in Fig. 8(a). The conspicuous effects of red tides are the associated wildlife mortalities among marine and coastal species of fish, birds, marine mammals and other organisms. Thus, several mobile sensor nodes are deployed to monitor the red tide on the sea surface and warn unaware entities from the dangerous zone.

The red tide zone is defined as a boundary in which the density of Alexandrium cells (one kind of red tide) are above 90 mg/L. The maximum area of this zone is 1002400m<sup>2</sup> and

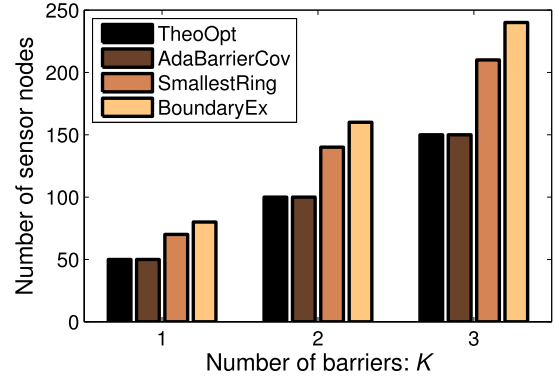


Fig. 9. The number of sensor nodes needed to form the different number of barriers  $K$ .

the maximum length of this region is 8220m. This red tide zone moves and deforms itself because of many factors, such as ocean current and wind. The maximum velocity of the red tide region is 1.296 km per day (0.015m/s average).

In simulations, 100 sensor nodes are adopted by default. The sensing range is set as  $r_s = 50$ m and the safety distance is set as  $\epsilon = 30$ m. The movement parameters used for our mobile sensor nodes refer to the Starborg AUV [8], which is one small unmanned water vehicle. The velocity of this sensor node is up to 1.5m/s. The battery allows this sensor node continuously moving up to 7500m.

We compare the performance of our *adaptive barrier coverage system* (AdaBarrierCov) with the *theoretical optimum* (TheoOpt), the *boundary extension coverage* (BoundaryEx) and the *smallest ring coverage* (SmallestRing). The TheoOpt is calculated according to the theoretical analysis in Section 4, which assumes that the trace of red tide is pre-known. The BoundaryEx forms the sensor nodes to be the  $\epsilon$ -boundary extension of the dynamic zone as the dot line in Fig. 7(a). In SmallestRing, the sensor nodes always move to construct a smallest ring shape containing the dynamic zone.

### B. Performance Results

In Fig. 8(b) and (c), the discrete points represent the positions of sensor nodes and the black area represents the red tide zone. These figures show two snapshots of the zone and 100 mobile sensor nodes. We find that the sensor nodes form a chain as the extended convex hull of the zone, and the intervals between neighbors are almost equal.

Fig. 9 shows the relation between the number of barriers  $K$  and the number of necessary sensor nodes when the region is as shown in Fig. 8(c). In this case, the length of the 30-extension convex hull is 4965m, the 30 boundary extension is 7650m and the smallest ring is 7008m. As shown in Fig. 9, to achieve  $K = 1$ , both TheoOpt and AdaBarrierCov need 50 nodes, but SmallestRing and BoundaryEx need 71 and 77 nodes respectively. These numbers linearly increase with the growth of  $K$ . We observe that our AdaBarrierCov can achieve the optimal  $\max(K)$  and is better than the other solutions.

Fig. 10 plots the distribution of the number of barriers  $K$  of different methods over time. The theoretical optimal number of barriers varies with the change of the red tide zone, where

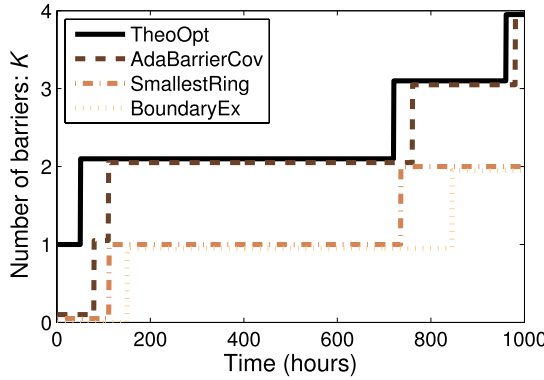


Fig. 10. The distribution of the number of barriers over time.

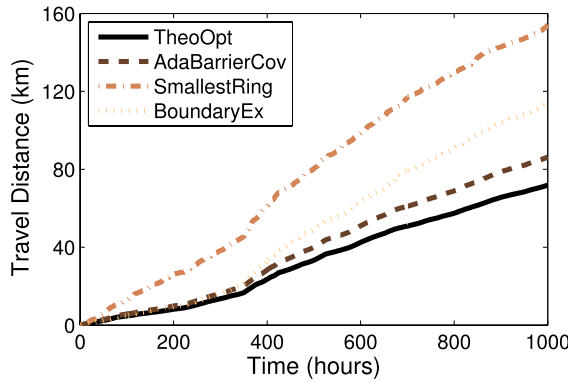


Fig. 11. The total travel distance of all sensor nodes with time.

TABLE I

MAXIMUM VELOCITY REQUIRED BY DIFFERENT METHODS  
WHEN THE VELOCITY OF ZONE IS  $v_z = 0.015\text{m/s}$

	Maximum Velocity Requirement
AdaBarrierCov	0.015m/s
BoundaryEx	0.015m/s
SmallestRing	0.028m/s

there are 43 hours with  $K = 1$ , 661 hours with  $K = 2$ , 257 hours with  $K = 3$  and 39 hours with  $K = 4$ . In our AdaBarrierCov, there are 79 hours with  $K = 0$ , 32 hours with  $K = 1$ , 627 hours with  $K = 2$ , 233 hours with  $K = 3$  and 29 hours with  $K = 4$ . Since the AdaBarrierCov consumes time on a process of sensing, communication, computing, and moving, its result has a little delay compared with the TheoOpt, which assumes the trace of red tide is pre-known. In addition, AdaBarrierCov performs much better than BoundaryEx and SmallestRing, whose performance even cannot reach  $K = 3$ .

The total travel distance over time is shown in Fig. 11 to assess the energy consumption. The shorter travel distance indicates the lower energy consumption, which is important for mobile monitoring. In Fig. 11, the travel distance in AdaBarrierCov is close to the optima and is much smaller than other two. At the end of simulation time, AdaBarrierCov, BoundaryEx and SmallestRing move 12.18%, 47.19% and 104.69% distance more than the TheoOpt. The total travel distance of AdaBarrierCov is 84122m and every sensor node

moves 841.22m in average. In all sensor nodes, the longest one moves about 1139.45m. Such a travel distance is practical since a Starburg AUV can move up to 7500m.

In Table 1, we measure the maximum velocity required by different methods when the red tide zone moves at a velocity of  $0.015\text{m/s}$ . It is sufficient for both AdaBarrierCov and BoundaryEx that the sensor nodes move as fast as the dynamic zone. However, the SmallestRing needs a greater velocity since it has to maintain sensor nodes as a ring.

## VII. CONCLUSION

This paper studies the adaptive barrier coverage for dynamic zones. We formulate this problem and derive the theoretical maximum number of barriers. Then, we proposed a software defined system consisting of the cloud-based architecture and the barrier maintenance algorithm. The cloud-based architecture provides high computation capability and global view. And the proposed algorithm imitates an elastic band, which continuously retains the barrier coverage wrapping the dynamic zone. Thus, our system approaches the maximum number of barriers for high monitoring quality and effectively reduces the total travel distance for energy saving. In addition, the software defined system provides the opportunity of sustainable development. More strategies can be easily added if more practical factors need to be taken into account.

## REFERENCES

- [1] A. R. Al-Ali, I. Zualkernan, and F. Aloul, "A mobile GPRS-sensors array for air pollution monitoring," *IEEE Sensors J.*, vol. 10, no. 10, pp. 1666–1671, Oct. 2010.
- [2] A. Chen, S. Kumar, and T. H. Lai, "Designing localized algorithms for barrier coverage," in *Proc. ACM MobiCom*, 2007, pp. 63–74.
- [3] J. Chen, J. Li, and T. H. Lai, "Energy-efficient intrusion detection with a barrier of probabilistic sensors: Global and local," *IEEE Trans. Wireless Commun.*, vol. 12, no. 9, pp. 4742–4755, Sep. 2013.
- [4] M. Chen, Y. Zhang, L. Hu, T. Taleb, and Z. Sheng, "Cloud-based wireless network: Virtualized, reconfigurable, smart wireless network to enable 5G technologies," *Mobile Netw. Appl.*, vol. 20, no. 6, pp. 704–712, Dec. 2015.
- [5] M. Chen, Y. Zhang, Y. Li, S. Mao, and V. C. M. Leung, "EMC: Emotion-aware mobile cloud computing in 5G," *IEEE Netw.*, vol. 29, no. 2, pp. 32–38, Mar./Apr. 2015.
- [6] W.-P. Chen, J. C. Hou, and L. Sha, "Dynamic clustering for acoustic target tracking in wireless sensor networks," *IEEE Trans. Mobile Comput.*, vol. 3, no. 3, pp. 258–271, Jul. 2004.
- [7] J. Du, K. Wang, H. Liu, and D. Guo, "Maximizing the lifetime of  $k$ -discrete barrier coverage using mobile sensors," *IEEE Sensors J.*, vol. 13, no. 12, pp. 4690–4701, Dec. 2013.
- [8] M. Dunbabin, J. Roberts, K. Usher, G. Winstanley, and P. Corke, "A hybrid AUV design for shallow water reef navigation," in *Proc. IEEE ICRA*, Apr. 2005, pp. 2105–2110.
- [9] S. He, J. Chen, X. Li, X. S. Shen, and Y. Sun, "Mobility and intruder prior information improving the barrier coverage of sparse sensor networks," *IEEE Trans. Mobile Comput.*, vol. 13, no. 6, pp. 1268–1282, Jun. 2014.
- [10] S. He, X. Gong, J. Zhang, J. Chen, and Y. Sun, "Curve-based deployment for barrier coverage in wireless sensor networks," *IEEE Trans. Wireless Commun.*, vol. 13, no. 2, pp. 724–735, Feb. 2014.
- [11] H. Kim and N. Feamster, "Improving network management with software defined networking," *IEEE Commun. Mag.*, vol. 51, no. 2, pp. 114–119, Feb. 2013.
- [12] L. Kong, X. Liu, Z. Li, and M.-Y. Wu, "Automatic barrier coverage formation with mobile sensor networks," in *Proc. IEEE ICC*, May 2010, pp. 1–5.
- [13] L. Kong *et al.*, "Surface coverage in sensor networks," *IEEE Trans. Parallel Distrib. Syst.*, vol. 25, no. 1, pp. 234–243, Jan. 2014.

- [14] S. Kumar, T. H. Lai, and A. Arora, "Barrier coverage with wireless sensors," in *Proc. ACM MobiCom*, 2005, pp. 284–298.
- [15] B. Liu, O. Dousse, P. Nain, and D. Towsley, "Dynamic coverage of mobile sensor networks," *IEEE Trans. Parallel Distrib. Syst.*, vol. 24, no. 2, pp. 301–311, Feb. 2013.
- [16] X.-Y. Liu, K.-L. Wu, Y. Zhu, L. Kong, and M.-Y. Wu, "Mobility increases the surface coverage of distributed sensor networks," *Comput. Netw.*, vol. 57, no. 11, pp. 2348–2363, 2013.
- [17] H. Mostafaei and M. R. Meybodi, "An energy efficient barrier coverage algorithm for wireless sensor networks," *Wireless Pers. Commun.*, vol. 77, no. 3, pp. 2099–2115, 2014.
- [18] B. A. A. Nunes, M. Mendonca, X.-N. Nguyen, K. Obraczka, and T. Turletti, "A survey of software-defined networking: Past, present, and future of programmable networks," *IEEE Commun. Surveys Tuts.*, vol. 16, no. 3, pp. 1617–1634, Aug. 2014.
- [19] C. Perera, A. Zaslavsky, C. H. Liu, M. Compton, P. Christen, and D. Georgakopoulos, "Sensor search techniques for sensing as a service architecture for the Internet of Things," *IEEE Sensors J.*, vol. 14, no. 2, pp. 406–420, Feb. 2014.
- [20] R. T. Rockafellar, *Convex Analysis*, Princeton, NJ, USA: Princeton Univ. Press, 2015.
- [21] A. Saipulla, C. Westphal, B. Liu, and J. Wang, "Barrier coverage of line-based deployed wireless sensor networks," in *Proc. IEEE INFOCOM*, Apr. 2009, pp. 127–135.
- [22] D. W. Townsend, N. R. Pettigrew, and A. C. Thomas, "Offshore blooms of the red tide dinoflagellate, *Alexandrium* sp., in the gulf of maine," *Continental Shelf Res.*, vol. 21, no. 4, pp. 347–369, 2001.
- [23] B. Wang, J. Chen, W. Liu, and L. T. Yang, "Minimum cost placement of bistatic radar sensors for belt barrier coverage," *IEEE Trans. Comput.*, vol. 65, no. 2, pp. 577–588, Feb. 2015.
- [24] Z. Wang, J. Liao, Q. Cao, H. Qi, and Z. Wang, "Achieving k-barrier coverage in hybrid directional sensor networks," *IEEE Trans. Mobile Comput.*, vol. 13, no. 7, pp. 1443–1455, Jul. 2014.
- [25] Z. Wang *et al.*, "Cyber-physical systems for water sustainability: Challenges and opportunities," *IEEE Commun. Mag.*, vol. 53, no. 5, pp. 216–222, May 2015.
- [26] G. Yang and D. Qiao, "Multi-round sensor deployment for guaranteed barrier coverage," in *Proc. IEEE INFOCOM*, Mar. 2010, pp. 1–9.
- [27] Z. Yu, F. Yang, J. Teng, A. C. Champion, and D. Xuan, "Local face-view barrier coverage in camera sensor networks," in *Proc. IEEE INFOCOM*, Apr./May 2015, pp. 684–692.
- [28] Y. Zhang, M. Chen, S. Mao, L. Hu, and V. Leung, "CAP: Community activity prediction based on big data analysis," *IEEE Netw.*, vol. 28, no. 4, pp. 52–57, Jul./Aug. 2014.
- [29] Y. Zhang, M. Qiu, C.-W. Tsai, M. M. Hassan, and A. Alamri, "Health-CPS: Healthcare cyber-physical system assisted by cloud and big data," *IEEE Syst. J.*, to be published.
- [30] Y. Zou and K. Chakrabarty, "Sensor deployment and target localization based on virtual forces," in *Proc. IEEE INFOCOM*, vol. 2, Mar. 2003, pp. 1293–1303.

**Linghe Kong** received the B.E. degree in automation from Xidian University in 2005, the Dipl.-Ing. degree in telecommunication from TELECOM SudParis in 2007, and the Ph.D. degree in computer science from Shanghai Jiao Tong University in 2012. From 2014 to 2015, he was a Post-Doctoral Fellow with the School of Computer Science, McGill University. He is currently an Associate Professor with Shanghai Jiao Tong University. His research interests include wireless sensor networks, mobile computing, and RFID.

**Siyu Lin** received the B.E. and Ph.D. degrees in electronics engineering from Beijing Jiaotong University, Beijing, China, in 2007 and 2013, respectively. From 2009 to 2010, he was an Exchange Student with the Universidad Politecnica de Madrid, Madrid, Spain. From 2011 to 2012, he was a Visiting Student with the University of Victoria, VIC, BC, Canada. He has been an Assistant Professor with Beijing Jiaotong University since 2013. His main research interests include performance analysis and channel modeling for wireless communication networks.

**Weiliang Xie** received the B.E. and M.E. degrees in information science and technology from Nankai University, and the Ph.D. degree in information science and technology from Peking University, China. He is currently a Professorate Senior Engineer with China Telecom Corporation Ltd. His research interests cover mobile network and wireless communication system.

**Xiaoyu Qiao** received the B.E. and Ph.D. degrees in electronics engineering from Beijing Jiaotong University, China, in 2007 and 2013, respectively. From 2011 to 2012, she was a Visiting Student with the University of California, Davis, CA, USA. She is a Senior Engineer with China Telecom Corporation Ltd. Her research interests cover mobile network and wireless communication system.

**Xi Jin** received the M.S. and Ph.D. degrees in computer science from Northeastern University, Shenyang, Liaoning, China, in 2008 and 2012, respectively. She is currently an Associate Professor with the Shenyang Institute of Automation, Chinese Academy of Sciences. Her research interests include wireless sensor networks and real-time systems.

**Peng Zeng** received the Ph.D. degree from the Shenyang Institute of Automation, Chinese Academy of Sciences. He is currently a Professor with the Shenyang Institute of Automation, Chinese Academy of Sciences. His research interests include industrial communication and wireless sensor networks.

**Wanli Ren** received the B.S. degree in computer science and technology from Yanshan University. He is currently pursuing the M.E. degree with Beijing Jiaotong University, China. His major study focuses on wireless sensor networks.

**Xiao-Yang Liu** received the B.Eng. degree in computer science from the Huazhong University of Science and Technology, China, in 2010. He is currently pursuing the Ph.D. degree with the Department of Computer Science, Shanghai Jiao Tong University. He is currently an Engineer with Shanghai Jiao Tong University. His research interests include sparse optimization, tensor theory and deep learning, wireless communication, distributed systems, and big data analysis and cyber security.